Blind Deconvolution Algorithm for Spatially-Invariant Motion Blurred Images based on Inverse Filtering and DST

Wikky Fawwaz Al Maki and Sueo Sugimoto

***Abstract*—**In this paper, a blind deconvolution algorithm for spatially-invariant motion blurred images is discussed. To obtain the sharp images, the point spread function is estimated. For the linear motion blur case, it is sufficient to estimate the motion length and the motion direction. The parameters are estimated by using the modified Radon transform and power cepstrum analysis. The blurred images are restored by using a DST-based deconvolution method and the spatial domain-based inverse filtering. Experimental results show our proposed ideas.

***Keywords*—**Blind image deconvolution. discrete sine transformation, inverse filter, modified Radon transform, motion blur.

I. Introduction

Motion blur is one of the most common causes of the image degradation. Motion blur occurs when there is a relative motion between the camera and the captured objects. Motion blur is an undesired effect that decreases resolution of an image mostly in the motion direction. To obtain the sharp images, various image deconvolution method can be applied. In the classical image deconvolution method, the point spread function (PSF) is given and the degradation process is inverted using one of the known algorithms such as least-square filtering, recursive Kalman filter, and constrained deconvolution method [1]-[4] However, in practical situations, the point spread function is unknown. It leads to the blind image deconvolution problem.

There are two important problems in the blind restoration of images degraded by the linear motion blur: identification of parameters of the point spread function and deconvolution of the blurred images. In the linear motion blur case, the point spread function has two important parameters, i.e. motion direction and motion length. The image deconvolution is performed using the identified motion direction and motion length. Since the success of the deconvolution of linear motion blurred images depends on the accuracy of the estimated parameters, robustness of the estimation methods are very important to consider.

Estimation of parameters of the point spread function plays important role in restoring the degraded image successfully. Many researchers have tried to solve this problem. The proposed algorithms were different in capability, accuracy, computational cost, etc. In [5], [6], bispectrum is used in blur identification. Estimation of parameters of the point spread function using cepstral analysis is presented in [4], [7], [8]. The recent works are presented in [9], [10]. In [10], Fuzzy sets and the Radon transform are used to identify the PSF. When motion length is small, the accuracy of motion direction estimation using the Radon transform will decrease. The Radon transform often fails in this case.

In [9], 1-D cepstral analysis and the Hough transform are demonstrated. The Hough transform needs candidate points [10]. Performance of the Hough transform for small length becomes less. Moreover, since the estimated motion direction is used to rotate the Fourier spectrum image, the accuracy of motion length estimation will be affected. 1-D cepstral analysis does not give better result than 2-D if we measure the motion length directly from the origin. In this paper, an algorithm to identify parameters of the point spread is proposed. Once the parameters of the point spread function have been estimated, the remaining problem is the deconvolution of the blurred image.

There are various image restoration methods that address motion blurred image. The image deconvolution methods have various capabilities and limitations. Many researchers apply the iterative techniques. However, the iterative techniques need more computational time [11]. The most well-known fast algorithms for image restoration involve the use of fast Fourier transform (FFT) to implement shift-invariant deblurring operators [12]. However, ringing artifact usually appears in the estimated true image. Therefore, we apply spatial domain-based deconvolution methods to obtain the sharp images.

II. PSF and Blurred Image Model

The point spread function of linear motion blur in spatial domain can be modeled as

$$h(x, y) = \frac{1}{L}\,\mathrm{rect}(v) \qquad ; v = x\cos\theta + y\sin\theta \tag{1}$$

Manuscript received November 9, 2006; Revised April 13, 2007

Wikky Fawwaz Al Maki is with Department of Electrical and Electronic Engineering, Ritsumeikan University, Japan (phone: +81-77-566-1111 ext. 8538; fax: +81-77-561-2663; e-mail: gr045058@se.ritsumei.ac.jp).

Sueo Sugimoto is with Department of Electrical and Electronic Engineering, Ritsumeikan University, Japan (phone: +81-77-566-1111 ext. 8123; fax: +81-77-561-2663; e-mail: sugimoto@se.ritsumei.ac.jp).

where *rect(v)* is given by

$$\text{rect(v)} = \begin{cases} 1/\text{L} & \text{if} \quad |v| \le \dfrac{L}{2} \\ 0 & \text{if} \quad |v| > \dfrac{L}{2} \end{cases}$$

From (1), it is obvious that the point spread function of linear motion blur has two parameters: motion length (L) and motion direction (θ). Equation (1) concludes that the point spread function of linear motion blur is equal to zero, except along a line that has an angle θ with x-axis and length L. If (1) is written in term of delta function (δ), then the point spread function of linear motion blur for any angle can be expressed as

$$\text{h(x, y)} = \frac{1}{\text{L}} \int_{-\text{L}/2}^{\text{L}/2} \delta(\text{x} - \text{t}\cos\theta)\,\delta(\text{y} - \text{t}\sin\theta)\,\text{dt} \tag{2}$$

The point spread function of linear motion blur is a low pass filter. If it is convolved with an image, it will act as convolution kernel those low-passes the image in the direction of the motion blur.

In frequency domain, the PSF of linear motion blur is given by [13]

$$\text{H}(\xi_1, \xi_2) = \text{sinc}(\pi\text{L}(\xi_1\cos\theta + \xi_2\sin\theta)) \tag{3}$$

where (ξ_1, ξ_2) represents the spatial Fourier coordinates. Equation (3) shows that parameters of the PSF are maintained in the frequency domain representation. If the frequency response shown in (3) is displayed as an intensity image, there will be parallel lines that show the sinc structure. Width and direction of the lines has strong relation with the motion length (L) and the motion direction (θ), respectively.

Since the PSF is linear spatially-invariant, the blurred image is modeled as an output of convolution between the true image *f(x, y)* and the point spread function *h(x, y)*:

$$\text{g(x, y)} = \text{h(x, y)} * \text{f(x, y)} \tag{4}$$

In continuous form, (4) is expressed as

$$\text{g(x, y)} = \int_{-\infty}^{\infty}\int_{-\infty}^{\infty} \text{h}(\zeta, \eta)\,\text{f}(\text{x} - \zeta, \text{y} - \eta)\,\text{d}\zeta\text{d}\eta \tag{5}$$

Equation (5) can be written in discrete domain as

$$\text{g(m, n)} = \sum_{\text{p}=-\text{P}}^{\text{P}} \sum_{\text{q}=-\text{Q}}^{\text{Q}} \text{h}_{\text{p,q}}\,\text{f}(\text{m} - \text{p}, \text{n} - \text{q}) \tag{6}$$

Since convolution in the spatial domain is equal to multiplication in the frequency domain, (5) can be written as

$$\text{G}(\xi_1, \xi_2) = \text{F}(\xi_1, \xi_2)\,\text{H}(\xi_1, \xi_2) \tag{7}$$

III. PSF Paramaters Estimation

Estimation of parameters of the PSF is performed by using the Fourier spectrum of the blurred image. The spectrum of the blurred image is anisotropic, shown by parallel lines whose direction is perpendicular to the direction of motion blur. Direction of these lines can be identified using a line detection algorithm, such as the modified Radon transform. Sinc structure, shown by the parallel lines, has periodicity indicated by location of spectral zeros. The motion length can be estimated by observing spectral zeros.

A. Motion Length Estimation

If the PSF is spatially variant, its parameters should be estimated in spatial domain [14], [15]. Since the PSF of the linear motion blur is spatially invariant, the spectral zeros or zero crossings can be identified in spectral domain. For the linear motion blur case, the motion length and the motion direction can be estimated from the spectral zeros in the frequency response.

Let *g(x, y)*, *h(x, y)*, and *f(x, y)* denote the blurred image, the point spread function, and the original image, respectively. If the blurred image is noiseless, then a power density spectrum of the blurred image is defined as [4]

$$\left|\text{G}(\xi_1, \xi_2)\right|^2 = \left|\text{F}(\xi_1, \xi_2)\right|^2 \left|\text{H}(\xi_1, \xi_2)\right|^2 \tag{8}$$

If the images *g(x, y)* and *f(x, y)* are divided into non overlapping sub-images $g_k(x, y)$, $f_k(x, y)$; k= 1, 2, ..., K, the power density spectra of these sub images will approximately satisfy relation similar to (8) [4]

$$\left|\text{G}_\text{k}(\xi_1, \xi_2)\right|^2 = \left|\text{F}_\text{k}(\xi_1, \xi_2)\right|^2 \left|\text{H}(\xi_1, \xi_2)\right|^2 \tag{9}$$

Taking algorithms of both sides of (8) and adding the results for each of the sub images gives [4]

$$\frac{1}{\text{K}}\sum_{\text{k=1}}^{\text{K}} \log\left|\text{G}_\text{k}(\xi_1, \xi_2)\right|^2 \approx \frac{1}{\text{K}}\sum_{\text{k=1}}^{\text{K}} \log\left|\text{F}_\text{k}(\xi_1, \xi_2)\right|^2 + \log\left|\text{H}(\xi_1, \xi_2)\right|^2$$

The first sum on the right side of could be approximated by an average power spectrum evaluated over a wide variety of images [16]. Magnitude response of the PSF can be estimated from the expression on the left-hand side of the aforesaid formula. An alternative to the above for identifying linear motion blur involves the computation of the 2-D power cepstrum of *g(x, y)* [4]. The power cepstrum used to estimate parameters of the PSF is given by

$$\text{g}_\tau = \Im^{-1}\{\log|\,\text{G}(\xi_1, \xi_2)\,|\} \tag{10}$$

In noiseless blurred image case, the power cepstrum of the blurred image is given by

$$\text{g}_\tau(\text{x, y}) = \text{f}_\tau(\text{x, y}) + \text{h}_\tau(\text{x, y}) \tag{11}$$

If $n = \xi_1\cos\theta + \xi_2\sin\theta$, (6) concludes as

$$\text{H}(\xi_1, \xi_2) = \text{sinc}(\pi\,\text{L}\,\text{n}) \tag{12}$$

The response has zeros at $n = m/L$, where $m = 0, 2, 3, \ldots$ As a result, $h_\tau(x, y)$ has a large negative spike at a distance L from the origin. Therefore, the motion length is identified by calculating the distance of the large negative spike from the origin.

B. Motion Direction Estimation

Motion direction is estimated using the modified Radon transform and 2-D power cepstrum analysis. Motion direction estimation using power cepstrum analysis is performed by calculating the slope of a line connecting the origin to the large negative value of the cepstrum of the blurred image. We use both the modified Radon transform and the cepstral analysis in motion direction estimation.

The sharp edges of the image will cause additional lines in the spectral domain. The Radon transform will detect these edges. To avoid this effect, the boundaries of the image are smoothened out using a Gaussian window before estimating the motion direction. Since the values of the Gaussian windowed image will decay towards the image boundary, the edge effects disappear. Therefore, the blurred image is smoothened before PSF parameters estimation methods are applied.

The Radon transform of a function *f(x, y)*, denoted as $R(\rho, \theta)$, is defined as its line integral along a line inclined at an angle θ from the *y-axis* and at a distance ρ from the origin. The Radon transform is given by [17]

$$R(\rho,\theta)=\int_{-\infty}^{\infty}\int_{-\infty}^{\infty} f(x,y)\,\delta(x\cos\theta+y\sin\theta-\rho) \tag{13}$$

In the coordinate system (ρ, s), where

$$\begin{aligned}\rho &= x\cos\theta+y\sin\theta\\ s &= -x\sin\theta+y\cos\theta\end{aligned} \tag{14}$$

(13) can also be written as

$$R(\rho,\theta)=\int_{-\infty}^{\infty} f(\rho\cos\theta-s\sin\theta,\rho\sin\theta+s\cos\theta)\,ds \tag{15}$$

In order to apply the Radon transform on a 2-D digital image $g(m, n)$ of size MxN, discretization of the Radon transform must be considered. The discrete Radon transform discussed here is different from that has been proposed in [18]. To achieve the discrete Radon transform, continuous variables are sampled as follows [19].

$$\begin{aligned}&x = x_m = x_{min}+m, && m=0,1,...,M-1\\ &y = y_n = y_{min}+n, && n=0,1,...,N-1\\ &\theta=\theta_t=\theta_{min}+t\,\Delta\theta, && t=0,1,...,T-1\\ &\rho=\rho_r=\rho_{min}+r\,\Delta\rho && r=0,1,...,P_\theta-1\\ &s=s_k=s_{min}+k\,\Delta s, && k=0,1,...,S_{\rho,\theta}-1\end{aligned} \tag{16}$$

where

$$\begin{aligned}x_{min} &= -x_{max} = -(M-1)/2,\\ \rho_{min} &= -\rho_{max} = -\frac{(P_\theta-1)}{2}\Delta\rho,\\ y_{min} &= -y_{max} = -(N-1)/2,\\ s_{min} &= -s_{max} = -\frac{(S_{\rho,\theta}-1)}{2}\Delta s.\end{aligned} \tag{17}$$

In (16), θ_{min}, $\Delta\theta$, T, and $\Delta\rho$ are set to 0, π/T, π, and 1, respectively. In order to let all pixels of an image be utilized in the Radon transform for any angle θ, the values of Δs and P_θ are set as [19]

$$\Delta s=\begin{cases}\dfrac{1}{\sin\theta_t}, & \sin\theta_t > \sin\dfrac{\pi}{4}=\dfrac{1}{\sqrt{2}}\\[2ex] \dfrac{1}{|\cos\theta_t|}, & \sin\theta_t \le \sin\dfrac{\pi}{4}=\dfrac{1}{\sqrt{2}}\end{cases} \tag{18}$$

$$P_\theta \approx \lceil M\,\Delta s\rceil + 1 - (\lceil M\,\Delta s\rceil \bmod 2), \tag{19}$$

where P_θ is adjusted to take an odd integer value.

$S_{\rho,\theta}$ depends on both ρ and θ. If it is fixed and equal to M for some values of ρ, it will be arithmetically decreased in a series afterwards. Therefore, $S_{\rho,\theta}$ is determined by [19]

$$S_{\rho,\theta}\approx\begin{cases}M, & |\rho_r|\le\rho_{const}\\ M-[(|\rho_r|-\rho_{const})\,d] & |\rho_r|>\rho_{const}\end{cases} \tag{20}$$

In (20), ρ_{const} and d are given by [19]

$$\begin{aligned}\rho_{const} &= \left\lfloor \frac{M-1}{2}\left\|\cos\theta_t\right|-\left|\sin\theta_t\right|\right\rfloor,\\ d &= \frac{2(\alpha M-\beta)}{\alpha(\alpha-1)}.\end{aligned} \tag{21}$$

where

$$\begin{aligned}\alpha &= \left(\frac{P_\theta-1}{2}\right)-\rho_{const}+1,\\ \beta &= \frac{M^2}{2}-M\rho_{const}\end{aligned} \tag{22}$$

In (20) and (21), [.] denotes the rounding operation. If the Radon transform is applied to a digital image, the image pixels are not always exactly on the reference lines. Therefore, $S_{\rho,\theta}$ is approximated by assuming that each pixel is assigned to its nearest reference lines. The pixel position is determined by rounding operation as follows [19].

$$\begin{aligned}x_k' &= [\rho_r\cos\theta-s_k\sin\theta-x_{min}],\\ y_k' &= [\rho_r\sin\theta-s_k\cos\theta-x_{min}].\end{aligned} \tag{23}$$

By using (23), the discrete Radon transform of 2-D digital image is approximated from (15) as

$$R(\rho_r,\theta_t)\approx\Delta s\sum_{k=0}^{S_{\rho,\theta}} g(x_k',y_k') \tag{24}$$

In the discrete Radon transform given by (24), the number of pixels projected on a line is not necessarily the same for different directions and/or coordinates of a direction. Therefore, the summation of all coordinates along this line may not act in a similar statistical base for different parameters ρ and θ. To overcome this problem, the discrete Radon transform in (24) is modified using the sample mean [19].

Define a set $\Phi^{r,t}$, a slightly different from [19], as

$$\Phi^{r,t} = \{g(x_i', y_i') : \rho = \rho_r \text{ and } \theta = \theta_t, i = 0,1,...,S_{\rho,\theta} - 1\} \quad (25)$$

Using the aforesaid formula, (24) is rewritten as

$$R(\rho_r, \theta_t) = \Delta s \sum_{k=0}^{S_{\rho,\theta}-1} \Psi_k^{r,t}, \quad (26)$$

where $\Psi_k^{r,t}$, is the k^{th} element of the set $\Phi^{r,t}$.
Equation (26) can be written as

$$R(\rho_r, \theta_t) = \Delta s \, S_{\rho,\theta} \, \text{mean}(\Phi^{r,t}) \quad (27)$$

In the modified Radon transform, the summation in (26) is replaced by the sample mean. Therefore, (27) is written as

$$R(\rho_r, \theta_t) = \Delta s \ \text{mean}(\Phi^{r,t}) \quad (28)$$

By using the sample mean as shown above, a better performance for direction estimation is obtained because a more stabilized statistical behavior is obtained due to the different number of elements of the sets $\Phi^{r,t}$ [19].

In order to apply the discrete Radon transform, Fourier spectrum of blurred image is treated as an image. To find direction of the lines which appear in the spectrum, the Radon transform is calculated for all directions with θ. We compute the variance of the results for each direction, and then form the variance array V_A as

$$V_A(\theta_t) = \underset{\rho_r}{\text{Var}}[R(\rho_r, \theta_t)], \quad \theta_t \in \left[\pi - \frac{\pi}{180}\right] \quad (29)$$

The motion direction is obtained by finding the maximum value of variance array.

IV. Image Deconvolution

A. Inverse Filtering Method

Image deconvolution method discussed here is a spatial domain based-image deconvolution performed along the blurring path. To achieve this, (6) is reformulated to get 1-D degradation process. Therefore, the blurred image at m^{th} row is defined as

$$g_m(n) = \sum_{q=-Q}^{Q} h_q f_m(n-q) \quad (30)$$

In linear motion blurred case, (30) can be written as (31)

$$\begin{aligned} g_m(n) &= \sum_{l=-L/2}^{L/2} h_l f_m(n-l) \\ &= \sum_{l=0}^{L} \frac{1}{L} f_m(n-l) \end{aligned} \quad (31)$$

Equation (31) can be written in a matrix representation as

$$\mathbf{G_m} = \mathbf{H}\mathbf{F_m} \quad (32)$$

where $\boldsymbol{G_m} \in \Re^{Nx1}$, $\boldsymbol{H} \in \Re^{NxN}$, and $\boldsymbol{F_m} \in \Re^{Nx1}$ are defined by the following matrices.

$$\mathbf{G_m} = \begin{bmatrix} \mathbf{g(m,1)} \\ \mathbf{g(m,2)} \\ \vdots \\ \vdots \\ \mathbf{g(m,N)} \end{bmatrix} \qquad \mathbf{F_m} = \begin{bmatrix} \mathbf{f(m,1)} \\ \mathbf{f(m,2)} \\ \vdots \\ \vdots \\ \mathbf{f(m,N)} \end{bmatrix} \quad (33)$$

$$\mathbf{H} = \begin{bmatrix} \mathbf{h_0} & & & & & \mathbf{0} \\ \mathbf{h_1} & \ddots & & & & \\ \vdots & \ddots & \ddots & & & \\ \mathbf{h_{L-1}} & \cdots & \cdots & \mathbf{h_0} & & \\ & \ddots & \ddots & \ddots & \ddots & \\ \mathbf{0} & & \mathbf{h_{L-1}} & \cdots & \mathbf{h_1} & \mathbf{h_0} \end{bmatrix} \quad (34)$$

In (33), all matrix elements are 1/*L*. From (32), the estimated true image is obtained by applying (35) to each row, i.e. *m=1, 2,…, M*. Thus,

$$\hat{\mathbf{F}}_\mathbf{m} = \mathbf{H}^{-1}\mathbf{G_m} \quad (35)$$

$\boldsymbol{H^{-1}}$ in (35) is computed by applying elementary row operations. The restored image is then defined as

$$\hat{\mathbf{F}} = \begin{bmatrix} \hat{\mathbf{F}}_\mathbf{1}^\mathbf{T} \\ \hat{\mathbf{F}}_\mathbf{2}^\mathbf{T} \\ \vdots \\ \vdots \\ \hat{\mathbf{F}}_\mathbf{M}^\mathbf{T} \end{bmatrix} \quad (36)$$

where $\hat{\mathbf{F}}$ is an $M \times N$ matrix.

As for the motion blurred image with $0 < \theta < \pi/2$, (6) is redefined as

$$z(i,j) = \sum_{p=-P}^{P} \sum_{q=-Q}^{Q} h_{p,q} \, u(i-p, j-q) \quad (37)$$

where *u(i,j)* is the interpolated pixel obtained from the original image *F(m,n)* given by (6) along the line at the motion direction. Therefore the size of *U* will not be equal to that of *F* anymore. If the size of *F* is *M x N*, then *U* is a matrix with size *I x J*. *I* is computed by

$$I = M + \lceil (\tan\theta(N-1)) \rceil \quad (38)$$

J should be carefully calculated. The image should be considered to have the size *M x N*.

For $N \leq M$:

$$J = \left\lfloor \frac{1}{\sin\theta} \{(N-1)\tan\theta\} \right\rfloor + 1 \quad (39)$$

For $N > M$:

$$J = \left\lfloor \frac{1}{\cos\theta}\{(N-1) - \vartheta\} \right\rfloor + 1 \tag{40}$$

where

$$\vartheta = \frac{1}{\tan\theta}\{((N-1)\tan\theta) - (I-1)\} \tag{41}$$

By using (38) - (41), the degradation process that happens at motion direction $0 < \theta < \pi/2$ can be treated as the degradation process in horizontal direction. From (37), the blurred image at i^{th} row is defined as

$$z_i(j) = \sum_{l=0}^{L} \frac{1}{L} u_i(j-l) \tag{42}$$

In matrix form, (42) can be written as

$$\mathbf{Z_i} = \mathbf{H}\mathbf{U_i} \tag{43}$$

where $\mathbf{H} \in \Re^{JxJ}$ is defined in the same way as shown in (34). $\mathbf{Z_i} \in \Re^{Jx1}$ and $\mathbf{U_i} \in \Re^{Jx1}$ are defined by the following matrices.

$$\mathbf{Z_i} = \begin{bmatrix} \mathbf{z(i,1)} \\ \mathbf{z(i,2)} \\ \vdots \\ \vdots \\ \mathbf{z(i,J)} \end{bmatrix} \qquad \mathbf{U_i} = \begin{bmatrix} \mathbf{u(i,1)} \\ \mathbf{u(i,2)} \\ \vdots \\ \vdots \\ \mathbf{u(i,J)} \end{bmatrix} \tag{44}$$

If (45) is applied to each row of *Z*, i.e. i = 1, 2, …, *I*, then the restored image is obtained and is given by (46).

$$\hat{\mathbf{U}}_i = \mathbf{H}^{-1}\mathbf{Z}_i \tag{45}$$

$$\hat{\mathbf{U}} = \begin{bmatrix} \hat{\mathbf{U}}_1^T \\ \hat{\mathbf{U}}_2^T \\ \vdots \\ \vdots \\ \hat{\mathbf{U}}_I^T \end{bmatrix} \tag{46}$$

However, matrix $\hat{\mathbf{U}}$ is not the desired image. Each element of $\hat{\mathbf{U}}$ is an interpolated pixel along the line segment at the motion direction. Bilinear interpolation [20], [21] is applied to obtain the restored image, i.e, by re-interpolating the elements of $\hat{\mathbf{U}}$. For the motion blurred image with motion direction $\pi/2 < \theta < \pi$, (37) is reformulated as

$$z_{flip}(c,d) = \sum_{p=-P}^{P}\sum_{q=-Q}^{Q} h_{p,q} u_{flip}(c-p, d-q) \tag{47}$$

Matrix representation of (47) is given by

$$\mathbf{Z}_{flip} = \mathbf{H}\mathbf{U}_{flip} \tag{48}$$

where U_{flip} is a matrix obtained by performing matrix left-right flipping operation to the original image *F* and the interpolating *F* along a line segment at the motion direction. As a result, Z_{flip}, whose elements are $z_{flip}(c,d)$, is in a form of left-right flipped matrix. For an *M x N* original image *F*, the size of Z_{flip} is *C x D* [22]:

$$C = M + \lceil (\tan\varphi(N-1)) \rceil \tag{49}$$

For $N \le M$:

$$D = \left\lfloor \frac{1}{\sin\varphi}((N-1)\tan\varphi) \right\rfloor + 1 \tag{50}$$

For $N>M$

$$D = \left\lfloor \frac{1}{\cos\varphi}((N-1) - \kappa) \right\rfloor + 1 \tag{51}$$

where

$$\kappa = \frac{1}{\tan\varphi}\{((N-1)\tan\varphi) - (C-1)\} \tag{52}$$

In (49)-(52), $\varphi = \pi - \theta$.

By using the same way shown in (42) – (46), the true restored image can be obtained after matrix left-right flipping operation. To increase the quality of the restored image, the bilateral filter is applied. The bilateral filter is employed because it can preserve the image edges.

B. Discrete Sine Transformation Method

In this section, linear motion blur given by (1) is reformulated as shown in (53). Here, a point spread function for horizontal direction is considered. Let denote *T* as exposure time to record the image and *V* as relative speed, then the horizontal width of the point spread function is $VT = L_y = 2D_y+1$. Thus,

$$h(x,y) = a(y) = \begin{cases} \dfrac{1}{L_y}, & -\dfrac{L_y}{2} \le y \le \dfrac{L_y}{2} \\ 0, & \text{otherwise} \end{cases} \tag{53}$$

$$h_{k,l} = a_l = \int_{l-\frac{1}{2}}^{l+\frac{1}{2}} a(y)\,dy \tag{54}$$

The linear motion blurred image is defined as

$$z(i,j) = \sum_{k=-D_x}^{D_x}\sum_{l=-D_y}^{D_y} h_{k,l} u(i-k, j-l) \tag{55}$$

Since the motion direction is horizontal, by using the definition expressed in (54), (55) is reformulated as

$$z(i,j) = \sum_{l=-D_y}^{D_y} a_l u(i, j-l) \tag{56}$$

In matrix representation, (56) is written as

$$\underline{z}_i(i,j) = \tilde{A}\,\underline{u}_i, \qquad i = 1,2,...,M \tag{57}$$

where $\underline{z}_i \in \Re^{Nx1}$, $\underline{u}_i \in \Re^{Nx1}$, and $\tilde{A} \in \Re^{NxN}$ are defined as

$$\begin{aligned}\underline{\mathbf{z}}_i &= [\mathbf{z(i,1)} \quad \mathbf{z(i,2)} \quad \cdots \quad \mathbf{z(i,N)}]^T \\ \underline{\mathbf{u}}_i &= [\mathbf{u(i,1)} \quad \mathbf{u(i,2)} \quad \cdots \quad \mathbf{u(i,N)}]^T\end{aligned} \tag{58}$$

$$\tilde{\mathbf{A}} = \begin{bmatrix} \mathbf{a_0} & \cdots & \mathbf{a_{-D_y}} & & \mathbf{0} \\ \vdots & \ddots & & \ddots & \\ \vdots & & \ddots & & \mathbf{a_{-D_y}} \\ \mathbf{a_{D_y}} & & & \ddots & \vdots \\ & \ddots & & & \vdots \\ \mathbf{0} & & \mathbf{a_{D_y}} & \cdots & \mathbf{a_0} \end{bmatrix} \tag{59}$$

Therefore, $\underline{u}_i$ can be obtained by computing the inverse of matrix $\tilde{A}$ such that

$$\underline{\mathbf{u}}_i = \tilde{\mathbf{A}}^{-1}\underline{\mathbf{z}}_i\mathbf{(i,j)} \tag{60}$$

where usually $\tilde{A}^{-1}$ is obtained by the computational complexity of $O(N^3)$ multiplications. To reduce the computational complexity, discrete sine transform (DST) is used. The Toeplitz matrix $\tilde{A}$ can be decomposed as shown in (61) [23].

$$\tilde{A} = A + \hat{A} = \sum_{m=0}^{D_y} \alpha_m Q^m + \hat{A}, \tag{61}$$

where Q is a tridiagonal matrix and $\hat{A}$ is a Hankel matrix, namely

$$\mathbf{Q} = \begin{bmatrix} \mathbf{0} & \mathbf{1} & & \mathbf{0} \\ \mathbf{1} & \ddots & \ddots & \\ & \ddots & \ddots & \mathbf{1} \\ \mathbf{0} & & \mathbf{1} & \mathbf{0} \end{bmatrix} \tag{62}$$

and

$$\hat{\mathbf{A}} = \begin{bmatrix} \mathbf{a_2} & \cdots & \mathbf{a_{D_y}} & & \\ \vdots & \iddots & & & \\ \mathbf{a_{D_y}} & & \mathbf{0} & & \mathbf{a_{D_y}} \\ & & & \iddots & \vdots \\ & & \mathbf{a_{D_y}} & \cdots & \mathbf{a_2} \end{bmatrix} \tag{63}$$

In (61), α_m is given by

$$\alpha_m = \sum_{r=0}^{\left[\frac{K-m}{2}\right]} a_{2r+m,l}\beta_{r,m} \tag{64}$$

where

$$\beta_{r,m} = \begin{cases} 1; & \text{for} \quad r = 0 \\ (-1)^r \dfrac{2r+m}{r}\dbinom{m+r-1}{r-1}; & \text{for} \quad r = 1,\ldots,\left[\dfrac{K-m}{2}\right] \end{cases} \tag{65}$$

Then, the following well-known results of eigenvalues and eigenvectors are applied for the tridiagonal matrix Q such that A can be diagonalized by DST [23].

Eigenvalues and Eigenvectors of Q

The tridiagonal matrix Q is diagonalized by DST matrix such that we have the following relations [23]:

$$SQS = \Lambda_Q = \mathrm{diag}[\lambda_{Q,1}, \lambda_{Q,2}, \ldots, \lambda_{Q,N}] \tag{66}$$

$$\lambda_{Q,i} = 2\cos\frac{\pi i}{N+1}, \qquad 1 = 1,2,\ldots,N \tag{67}$$

where S is the following DST matrix whose row (or column) vectors are eigenvectors of Q corresponding to eigenvalues of $\{\lambda_{Q,i}\}$:

$$S = \left[\sqrt{\frac{2}{N+1}}\sin\frac{ij\pi}{N+1}\right] = S^T = S^{-1} \tag{68}$$

Therefore, from (61) and (66), we have [23]

$$SAS = \sum_{m=0}^{D_y} \alpha_m \Lambda_Q^m = \mathrm{diag}[\lambda_{A,1}, \ldots, \lambda_{A,N}] \tag{69}$$

where $\{\lambda_{A,i}\}$, i = 1,…, N, are eigenvalues of A and are given by

$$\lambda_{A,i} = \sum_{m=0}^{D_y} \alpha_m \lambda_{Q,i}^m = \sum_{m=0}^{D_y} \alpha_m \left(2\cos\frac{\pi i}{N+1}\right)^m, \; for \quad i = 1,2,..,N \tag{70}$$

Then, by applying DST to (57) with employing the relation in (61), we have

$$\mathbf{S}\underline{\mathbf{z}}_i = \mathbf{S(A + \hat{A})SS}\underline{\mathbf{u}}_i, \tag{71}$$

or

$$\underline{\mathbf{y}}_i = \mathbf{\Lambda}_A \underline{\mathbf{x}}_i + \mathbf{S\hat{A}S}\underline{\mathbf{x}}_i, \tag{72}$$

where $\underline{y}_i = S\,\underline{z}_i$ and $\underline{x}_i = S\,\underline{u}_i$. From (72), we can solve $\underline{x}_i$ by the following iteration method:

$$\underline{x}_i^{\,t} = \Lambda_A^{-1}(\underline{y}_i - S\hat{A}S\,\underline{x}_i^{\,t-1}), \qquad t = 1,2,\ldots \tag{73}$$

Next, from IDST ($S = S^{-1}$), $\{\underline{u}_i ; i = 1, \ldots, M\}$ is obtained, and the restored image is obtained [23].

V. Results and Discussion

Experiments are performed by using computer with specifications: Intel Pentium M 1.86 GHz and 1 GB RAM. The software used in the simulation is Matlab 6.5.1. To approach practical situation, an RGB image is used. Artificially blurred image is obtained by blurring simulation with angles varying from 0 to $\pi - \pi/180$ and length varying from 1-79 pixels. Before estimating the parameters of the PSF, the blurred image is windowed using a Gaussian window.

In this paper, the motion length (L) is estimated using only the 2-D power cepstrum analysis. However, in motion direction estimation (θ), two methods are used. As either the power cepstrum analysis and the modified Radon transform has different capabilities for a certain value of motion length, the two methods are used together. For L<14 pixels, the power

cepstrum analysis gives better motion direction estimation than the Radon transform does. The maximum error when we use the power cepstrum analysis is 3 degrees, but it becomes bigger if we use the modified Radon transform. For $L \geq 14$ pixels, the modified Radon transform can give better estimation than the power cepstrum analysis. Therefore, the estimated motion length obtained by the power cepstrum analysis is used to determine the better method to estimate the motion direction. If $L<14$ pixels, then the power cepstrum analysis is used to estimate the motion direction. If $L \geq 14$ pixels, the motion direction is estimated using the modified discrete Radon transform. The estimated parameters are then used in the image deconvolution to get the estimated true image. Table 1 shows the results of PSF parameters estimation. Performance of the image deconvolution method and the image smoothing method can also be verified from the table.

Table 1 PSF parameter estimation results for RGB image

L	θ	$\hat{L}$	$\hat{\theta}$	MSE_r	MSE_s
15	43	16	43	0.0541	0.0212
24	136	24	138	0.0380	0.0348
48	18	49	17	0.0467	0.0400
53	27	54	27	0.0316	0.0270
63	5	64	4	0.0283	0.0239

In Table 1, MSE_r denotes the mean square error computed using the restored image, and MSE_s denotes the mean square error computed using the restored image after image smoothing using the bilateral filter. The MSE is computed by

$$MSE = \frac{1}{MN}\sum_{m=0}^{M-1}\sum_{n=0}^{N-1}[\hat{f}(m,n) - f(m,n)]^2$$

where $\hat{f}(m,n)$ and $f(m,n)$ denote the restored image and the original image, respectively.

To show the capability of parameter identification and image deconvolution method, the original image, the blurred image, and the restored image are compared. Fig. 1, Fig. 2, Fig. 3, and Fig. 4 show the original image, the blurred image, the Gaussian-windowed blurred image, and the restored image (deconvolved image), respectively.

Fig. 1 Original image

Fig. 2 Motion blurred image (L=15 pixels, θ=43°)

Fig. 3 Gaussian-windowed motion blurred image

Fig. 4 Restored image using $\hat{L}$ =16 and $\hat{\theta}$ =43

Fig. 5 The restored image smoothed using bilateral filter

The experimental result for the use of DST is given as follows. In the simulation, the original image is blurred by linear motion blurred in horizontal direction with $L = 7$ pixels. The original image, the blurred image, and the restored image are shown by Fig. 6 – Fig. 8. Here, we use a monochrome image.

Fig. 6 Original Lenna Image

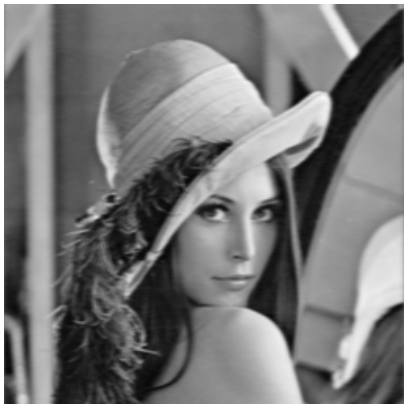

Fig. 7 Blurred Lenna Image (L = 7 pixels)

Fig. 8 Restored Image

The mean square error of the restored image (Fig. 8) is 4.6 x 10^{-25}. For linear motion blurred image with $\theta \neq 0^{o}$, after estimating L and θ, image is rotated θ degrees, and inverse filtering using DST is applied.

VI. Conclusion

PSF parameters estimation using the modified discrete Radon transform and the 2-D cepstral analysis has been demonstrated. Simulation results show the capability of the methods. The method of PSF parameter identification discussed here can be applied to any image size, any motion direction, and any motion length. By applying two methods which have their own capability, the accuracy of motion direction estimation using these methods is better than by just applying one of the methods. Restoring the blurred images using spatial domain-based image deconvolution method can avoid artifact which often happens in frequency domain-based image deconvolution method. To increase the quality of the restored image, bilateral filter is used. The advantage of this filter is the ability in preserving the edge of the image. This filter can improve the mean square error of the restored image. Image deconvolution using DST has given an acceptable result where the mean square error of the restored image is considerably small.

References

[1] T. Katayama, "Restoration of images degraded by motion blur and noise," in *Proc. 20th IEEE Conference on Decision and Control including the Symposium on Adaptive Processes*, San Diego, CA, 1981.

[2] A. K. Jain, S. Ranganath, "Applications of two dimensional spectral estimations in image restoration," in *Proc. IEEE Int. Conf. Acoustics, Speech, Signal Processing*, pp. 1113-1116, 1981.

[3] B. R. Hunt, "The application of constrained least square estimation to image restoration by digital computer," *IEEE Trans. Comput.*, vol. C-22. pp. 805-812, 1973.

[4] J. Biemond, R. L. Lagendijk, and R. M. Mersereau, "Iterative methods for image deblurring," in *Proc. IEEE*, pp. 856-883, 1990.

[5] M. M. Chang, A. M. Tekalp, A. T. Erdem, "Blur identification using the bispectrum," *IEEE Transaction on Signal Processing*, vol. 10, pp. 2323-2325, 1991.

[6] C. Mayntz, T. Aach, and D. Kunz, "Blur identification using a spectral inertia tensor and spectral zeros," in *Proc. IEEE International Conference on Image Processing*, 1999.

[7] M. Cannon, "Blind deconvolution of spatially invariant image blurs with phase," *IEEE Trans. Acoust. Speech Signal Process.*, vol.1, pp. 56-63, 1976.

[8] I. M. Rekleitis, "Optical flow recognition from the power spectrum of a single blurred image," in *Proc. IEEE International Conference on Image Processing*, 1996.

[9] R. Lokhande, K. V. Arya, P. Gupta, "Identification of parameters and restoration of motion blurred images," in *Proc. ACM Symposium on Applied Computing*, pp. 301-315, 2006.

[10] M. E. Moghaddam, M. Jamzad, "Motion blur identification in noisy images using fuzzy sets," in *Proc. IEEE International Symposium on Signal Processing and Information Technology*, Athens, 2005.

[11] D. Kundur, D. Hatzinakos,"Blind image deconvolution," IEEE Signal Proc. Magazine, 1996.

[12] H. C. Andrews, B. R. Hunt, Digital Image Restoration. New Jersey: Prentice Hall, 1977.

[13] W. F. Al Maki, H. Mori, T. Shimahashi, M. Matsubara, and S. Sugimoto, "Blind image restoration for motion blurred image", in *Proc. 51st SCI Conference on Control and Information Systems*, Kyoto, Japan, 2007.
[14] J. Biemond, F. G. Van der Putten, J. W. Woods, "Identification and restoration of images with symmetric non causal blurs," *IEEE Trans. Circ. Syst*., vol.1, pp. 385-393, 1988.
[15] A. M. Tekalp, H. Kaufman, J. W. Woods, "Identification of image and blur parameters for the restoration of non causal blurs," *IEEE Trans. Acoustics, Speech, Signal Process.*, vol. 34, pp. 963-972, 1986.
[16] T. G. Stockham, T. M. Cannon, R. B. Ingebretsen, "Blind deconvolution through digital signal processing," in *Proc. IEEE*, pp. 678-692, 1975.
[17] A. K. Jain, Fundamentals of digital image processing. New Jersey: Prentice Hall, 1989.
[18] P. Toft, "The Radon transform: Theory and implementation," Ph.D thesis, Technical University of Denmark, 1996.
[19] M. R. Hejazi, G. Shevlyakov, Y. S. Ho, "Modified discrete Radon transforms and their application to rotation-invariant image analysis," in *Proc. IEEE 8th Workshop on Multimedia Signal Processing*, pp. 429-434, 2006.
[20] R. C. Gonzalez, R. E. Wood, Digital image processing, 2nd edn. New Jersey: Prentice Hall, 2001.
[21] W. K. Pratt, Digital image restoration: PIKS inside, 3rd edn. New York: John Wiley and Sons, 2001.
[22] W. F. Al Maki, T. Shimahashi, M. Matsubara and S. Sugimoto, "PSF estimation and image restoration for noiseless motion blurred images," in *Proc. 7th WSEAS International Conference on Signal, Speech, Image Processing, Beijing, pp. 1-7,* 2007.
[23] S. Sugimoto, "Inverse filter and image enhancement from DFT to DST," in *Proc. 37th ISCIE Int. Symp. on Stochastic Systems Theory and Its Applications*, Osaka, pp. 54-59, 2005.

Wikky Fawwaz Al Maki was born in Garut (West Java, Indonesia) on November 25, 1982. He received B.Eng in electrical engineering in 2004 from the University of Indonesia, Depok, Indonesia, and M.Eng in electrical and electronic engineering in 2007 from Ritsumeikan University, Kusatsu, Shiga, Japan. Currently, he is a Ph.D student in Ritsumeikan University. He worked as a researcher in Science and Technology Research Center, the University of Indonesia, from 2004 to 2005. He became a Student Member of IEEE and ISCIE in 2007. His research interests are signal processing, image processing, stochastic systems, and visual optic.